Molecular and mineral responses of corals grown under artificial Calcite Sea conditions

Nicola Conci [1], Erika Griesshaber [1,4], Ramón E. Rivera-Vicéns [1], Wolfgang W. Schmahl [1,2,4], Sergio Vargas [1], Gert Wörheide [1,3,4] *

[1] Department of Earth and Environmental Sciences, Paleontology & Geobiology, Ludwig-Maximilians-Universität, Munich, Germany.
[2] SNSB - Mineralogische Staatssammlung, Munich, Germany
[3] SNSB - Bayerische Staatssammlung für Paläontologie und Geologie, Munich, Germany
[4] GeoBio-Center LMU, Ludwig-Maximilians-Universität, Munich, Germany

* corresponding author, email: woerheide@lmu.de

Abstract

The formation of skeletal structures composed of different calcium carbonate polymorphs (aragonite and calcite) appears to be regulated both biologically and environmentally. Among environmental factors influencing aragonite and calcite precipitation, changes in sea water conditions – primarily in the molar ratio of magnesium and calcium during so-called "Calcite" (*m*Mg:*m*Ca below 2) or "Aragonite" seas (*m*Mg:*m*Ca above 2) – have had profound impacts on the distribution and performance of marine calcifiers throughout the Earth's history. Nonetheless, the fossil record shows that some species appear to have counteracted such changes and kept their skeleton polymorph unaltered. Here, the aragonitic octocoral *Heliopora coerulea* and the aragonitic scleractinian *Montipora digitata* were exposed to Calcite Sea-like *m*Mg:*m*Ca with various levels of changes in magnesium and calcium concentration, and both mineralogical (i.e.,$CaCO_3$ polymorph) and gene expression changes were monitored. The two species exhibited different responses: no calcite deposition could be detected in *H. coerulea*, while *M. digitata* presented considerable amounts of calcite under *m*Mg:*m*Ca of 1.5. Nonetheless, aragonite was the main skeleton constituent in both species and under both treatment conditions. Despite a strong variability between experimental replicates, expression for a set of putative calcification-related genes, including known components of scleractinians skeleton organic matrix, was found to consistently change when *m*Mg:*m*Ca was lowered. These results are consistent with the hypothesis of an involvement of the skeleton organic matrix in counteracting decreases in seawater *m*Mg:*m*Ca. On the other hand, no clear changes in expression for calcium and magnesium transporters were detected. Nonetheless, different calcium channels were found downregulated in *H. coerulea* when exposed to *m*Mg:*m*Ca of 2.5, pointing to an active calcium uptake regulation by the corals under altered *m*Mg:*m*Ca to maintain aragonite deposition.

Introduction

Biomineralization refers to the process by which organisms deposit their skeletons. Anthozoan (Phylum Cnidaria) biomineralization holds a particularly important ecological role, as it represents the main mechanism sustaining the growth of coral reefs. In corals, skeletons are composed of different calcium carbonate ($CaCO_3$) polymorphs. Members of the order Scleractinia produce aragonite exoskeletons, with the sole exception of *Paraconotrochus antarcticus*, a recently discovered species that exhibits a two-component (i.e., aragonite and calcite) skeleton (Stolarski et al., 2021). In the subclass Octocorallia, an opposite pattern occurs: the vast majority of species produce calcitic endoskeletal structures, while aragonite exoskeletons are deposited by members of the order Helioporacea (i.e., the blue corals).

As observed in other organisms, including molluscs, arthropods and chordates, biomineralization in corals is a *biologically controlled* process (Lowenstam and Weiner, 1989). During biomineralization, corals control the availability and concentration of ions required for calcification (e.g., Ca^{2+} and HCO_3^-) in the extracellular calcifying medium (ECM) (Moya et al., 2008; Bertucci et al., 2011; Zoccola et al., 2015; Le Goff et al., 2016), and the production of various macromolecules putatively involved in calcium carbonate deposition, and collectively referred to as the skeleton organic matrix (SkOM). SkOM components are secreted into the calcification space and are eventually occluded within the skeleton mineral. Several regulatory functions have been attributed to the SkOM of corals and other marine calcifiers. These include crystal nucleation, formation and inhibition (Wheeler et al., 1981; Peled-Kamar et al., 2002; Puverel et al., 2005; Von Euw et al., 2017), and controlling the calcium carbonate ($CaCO_3$) polymorph of the skeleton (Thompson et al., 2000; Goffredo et al., 2011).

In corals, the effect of different organic compounds on $CaCO_3$ polymorphs (aragonite, calcite) has been investigated mostly through *in vitro* precipitation experiments. The addition of total SkOM extracts (Hohn and Reymond, 2019), or of proteins (Rahman and Oomori, 2009; Goffredo et al., 2011) and lipids (Reggi et al., 2016) isolated from coral skeletons to supersaturated $CaCO_3$ solutions, has been shown to promote or inhibit the formation of specific $CaCO_3$ polymorphs and to affect the shape of $CaCO_3$ crystals. Recently, Laipnik et al. (2019) observed that protein-driven *in vitro* precipitation of different $CaCO_3$ polymorphs is also related to the magnesium concentration ($[Mg^{2+}]$) in the solution used. In those experiments, the absence of aragonite formation – the naturally occurring polymorph in

scleractinian skeletons – at low magnesium concentrations led the authors to propose a key role for seawater [Mg^{2+}] in the functioning of coral skeletogenic proteins.

Seawater chemistry has in fact been long included among the main drivers of selective inorganic precipitation of different $CaCO_3$ polymorphs, with the molar ratio of magnesium and calcium (*m*Mg:*m*Ca) likely representing one of the key factors leading to differential $CaCO_3$ precipitation (Morse and Mackenzie, 1990; Morse et al., 1997; Balthasar and Cusack, 2015). From an evolutionary perspective, the *m*Mg:*m*Ca is particularly interesting due to its estimated fluctuations in the last 600 million years, which caused alternating periods of calcite- and aragonite-favouring oceanic environments (Sandberg, 1983) that robustly correlate with the preferred $CaCO_3$ skeleton polymorph of the dominant reef builders during those geological periods (Stanley and Hardie, 1998, 1999). During the Cretaceous, for example, when the *m*Mg:*m*Ca dropped to ~ 1 (compared to the modern value of 5.2), scleractinian corals were replaced by calcitic bivalves (rudists, Phylum Mollusca) as main reef builders. Remarkably, some calcitic scleractinians have been reported from this period (Stolarski et al., 2007). However, fossils of cretaceous aragonitic corals indicate that some coral species could deposit aragonite despite the lower, calcite-favouring *m*Mg:*m*Ca oceanic environment (Janiszewska et al., 2017). Aaragonitic blue coral fossils are also known from the Cretaceous (Eguchi, 1948; Colgan, 1984), further reinforcing the idea that the effect of different *m*Mg:*m*Ca ratios on the skeleton polymorph of corals differs between species and, likely, reflects the ability of some corals to deposit specific $CaCO_3$ polymorphs under chemically unfavourable conditions.

In vivo experiments exposing animals to different *m*Mg:*m*Ca ratios provide support for the ability of corals to counteract the putative decisive influence of seawater chemistry on polymorph formation. In an early work, Ries (2006) observed an increase in the amount of calcite present in the skeleton of three scleractinian corals, with the amount of calcite found correlating inversely to the seawater *m*Mg:*m*Ca ratio. These observations were later corroborated by Higuchi et al (2014), who reported significant amounts of calcite in the skeleton of juvenile *Acropora tenuis*, albeit at lower *m*Mg:*m*Ca ratios compared to Ries (2006). More recently, Yuyama et al. (2019) reported changes in gene expression in the scleractinian coral *A. tenuis* grown in Mg-depleted seawater. These included the up-regulation of several putative skeletogenic genes, suggesting that lower *m*Mg:*m*Ca elicits a response in the corals' calcification machinery. However, since Yuyama et al (2019) only manipulated the Mg-content of the water leaving the calcium levels constant, the molecular

response of corals to *m*Mg:*m*Ca ratios comparable to those observed during geological periods corresponding to Calcite Seas, when both the concentration of calcium and magnesium changed, remain unknown.

Here, we exposed the branching stony coral *Montipora digitata* (Scleractinia) and the blue coral *Heliopora coerulea* (Octocorallia) to both calcite and aragonite-inducing seawater and used gene expression analysis (RNA-seq), electron backscatter diffractometry (EBSD), and energy dispersive spectroscopy (EDS) to investigate the molecular and mineralogical response of these corals to different *m*Mg:*m*Ca ratios resembling past oceanic conditions. Our results indicate a higher tolerance to changes in *m*Mg:*m*Ca of octocorals compared to scleractinians and the involvement of several uncharacterized genes in the response of the corals to variations in mMg:mCa. For the blue coral, *H. coerulea*, we observed expression changes in genes involved in ion transport and ion availability while the expression of organic matrix proteins remained unaltered.

Materials and Methods

Fragments of *H. coerulea* and *M. digitata* were mechanically obtained from colonies cultured since more than a decade in the aquarium facilities of the Chair for Geobiology & Palaeontology of the Department of Earth and Environmental Sciences at Ludwig-Maximilians-Universität München (Munich, Germany). Following fragmentation, corals were allowed to recover for about one month prior to the start of each experiment. Two days before the start of each experiment, coral samples were incubated for ca. 36 hours in a 10% alizarin red solution to mark the skeleton deposited before the experiment.

Experimental Design

Two independent experiments were performed for each target species. Each experiment lasted ca. six weeks (22.07-10.09 and 01.11-12.12 2018 for *M. digitata* and 04.01-28.02 and 01.03-15.04 2019 for *H. coerulea)*. The experimental setup is illustrated in Figure 1. It consisted of three 8 L aquarium tanks: one (control tank) containing seawater with a *m*Mg:*m*Ca of 5.2 (10mM Ca^{2+} - 52 mM Mg^{2+}) and two treatment tanks with ratios 2.5 (17mM Ca^{2+}- 47 mM Mg^{2+}) and 1.5 (25mM Ca^{2+}- 37 mM Mg^{2+}). In all three tanks the sum of [Ca^{2+}] and [Mg^{2+}] was equal and set at 62 mmol. A single source of Mg^{2+} and Ca^{2+}-free seawater was used for all three tanks and the *m*Mg:*m*Ca ratio was adjusted by adding different amounts $CaCl_2xH_2O$ and $MgCl_2x6H_2O$ to each tank. Water was replaced in each tank every

2 days . Composition of control and treatment artificial seawater used is provided in S.Mat1 (available online at https://github.com/PalMuc/CalciteSea).

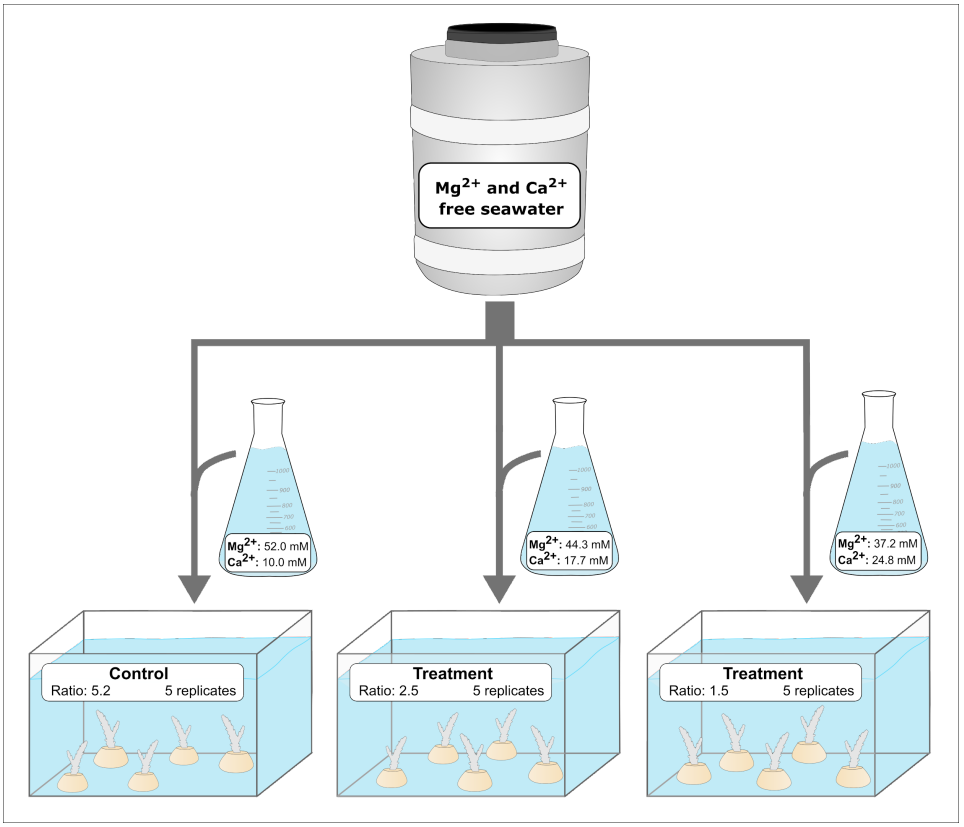

Figure 1 Schematic diagram of the experimental design. For each species the experiment was repeated twice: 22.07.-10.09.2018 and 01.11.-12.12.2018 for *M. digitata*, and 04.01.-28.02.2019 and 01.03.-15.04.2019 for *H. coerulea.*

To allow for acclimatisation, corals in treatment tanks were initially exposed for two days to a *m*Mg:*m*Ca ratio of 5.2, before lowering the *m*Mg:*m*Ca ratio to 4.0 and 3.0 for two days, respectively. After the acclimation phase, the *m*Mg:*m*Ca ratio was adjusted to the final experimental ratios. At the end of each experiment, one coral fragment was bleached for 24 hrs in 5% NaOCl, washed several times in ultrapure water, air dried and stored for mineralogical analysis. Three corals from each tank were flash frozen in liquid nitrogen and stored at -80° C until RNA extraction.

Mineralogical Analysis

To prepare coral samples for mineralogical analysis, skeletons were first thoroughly washed with deionized water and then air dried. Samples were embedded in polypropylene molds using ca. 30 ml of Epofix Resin (Struers) and 4 ml of Resin Hardener. Samples were placed in a vacuum desiccator to degas and polymerize for 24 hours. Embedded skeletons were grinded using P320, P600 and P1200 silicon carbide paper (Buehler), and flushed with

deionized water to remove resin and silicon residues. The first round of polishing was done with a 3 µm polycrystalline diamond suspension for ca. 10-15 minutes. The samples were then attached to cylinder weights with Thermoplastic Cement at 100-150°C. After reaching room temperature, samples were finally polished (for ca. three hours) with MicroFloc in a Vibromet using a 50 nm Alumina suspension, and washed. Prior to EBSD and EDS analysis, the polished samples were coated with 4-8 nm of carbon and mounted on a sample holder with a 70° tilt with respect to the beam. For each sample, an 'inner' and 'outer' area were analyzed to obtain mineralogical information of the skeleton deposited before and after the start of the experiment. EBSD and EDS measurements were performed with a Hitachi SU5000 field emission SEM operated at 20kV. The microscope is equipped with electron backscatter diffraction (EBSD) and energy dispersive spectroscopy (EDS) detectors (Oxford Instruments). Measurements were conducted using the AZtech Suite (Oxford Instruments), while phase and orientation maps were produced with the CHANNEL 5 HKL software (Schmidt and Olesen, 1989; Randle and Engler, 2000). Grains parameters for all samples were determined with Tango 5.12. For each mapped skeleton portion, relative abundance of grain area and major axis was computed. In an effort to account for differences possibly caused by sectioning plane and natural spatial heterogeneity of grain size, an additional variable "*minor axis"* was calculated by dividing each grain area by its major axis. For data plotting all three measures were log-transformed. Mineralogical datasets (both raw files and datasets with the additional variables) - alongside the R script used to generate the plots are provided in S.Mat 4 available at https://github.com/PalMuc/CalciteSea.

Transcriptome Sequencing

Coral samples were homogenised in 1-2 ml of Trizol (Thermofisher) using a Polytron PT Homogenizer (Kinematica) and centrifuged at 15,000 g for 10 minutes to remove residual skeleton powder. RNA was extracted according to a modified TriZol protocol (Chomczynski and Mackey, 1995). Modifications included the substitution of 50% of the isopropanol with a high-salt solution (1.2 M sodium chloride and 0.8 M sodium citrate) in order to avoid the coprecipitation of polysaccharides and other potential contaminants. RNA purity and integrity were assessed on a NanoDrop 2100 spectrophotometer and a Bioanalyzer 2100 (Agilent), respectively. For sequencing, only samples with a RIN value > 8.0 were considered. Strand-specific libraries were prepared with the SENSE mRNA-Seq Library Prep Kit V2 for Illumina (Lexogen) and paired-end sequenced (50 bp) on an Illumina HiSeq1500 at the Gene Center of Ludwig-Maximilians-Universität München.

Sequences were quality controlled with FastQC (www.bioinformatics.babraham.ac.uk) and low quality reads removed with the Filter Illumina program from the Agalma-Biolite transcriptome package (Q value cutoff: 28) (Dunn et al., 2013). Reads generated as part of these experiments have been deposited at the European Nucleotide Archive (www.ebi.ac.uk/ena) under Bioproject Number PRJEB36989 (*M. digitata*) and PRJEB36990 (*H. coerulea*). For the assembly of *H. coerulea,* previously sequenced reads (PRJEB30452) were also used.

Transcriptomes were assembled with TransPi (Rivera-Vicéns et al., 2022). Contigs of length < 300 bp were discarded. Host and symbiont contigs were separated with psytrans (https://github.com/sylvainforet/psytrans) using the *Dendronephthya gigantea* (Jeon et al. 2019) and *Acropora digitifera* (Shinzato et al., 2011) sequences for assigning host contigs of *H. coerulea* and *M. digitifera* sequences, respectively. Transcriptome completeness was assessed with BUSCO 3.0.2 (metazoa database) (Simão et al., 2015). Summary statistics of the transcriptomes are provided in Table 1.

Table.1 Summary statistics for the *H. coerulea* and *M. digitata* transcriptomes assembled with Transpi. Parameters refers to host transcriptome CDS only after contigs assignment with psytrans. For BUSCO scores, percentages of complete (C), fragmented (F) and missing (M) are provided.

Species	Contigs	N50 - Mean length	BUSCO [C-F-M]
H. coerulea	110,535	819 - 716	[97.0 - 1.4 - 1.6]
M. digitata	71,676	819 -705	[90.4 - 4.3 - 5.3]

Gene Expression Analysis

For gene expression analysis, read files of each species were mapped against their metatranscriptome (host and symbiont contigs) using Salmon 0.11.2 (Patro et al., 2017) via our local Galaxy server (galaxy.palmuc.org). Read quantification files for each sample were combined into a count matrix with the abundance_estimates_to_matrix.pl script provided with Trinity 2.8.6 (Grabherr et al., 2011) and count data for host (coral) sequences was filtered based on psytrans results. Differential expression analysis was performed using DESeq2 v.1.24.0 (Love et al., 2014). Presence of technical batch effects (Supplementary Figures C1 and C2) was included in the model for DESeq2 analysis using the design formula "*~experiment + condition*". For each comparison (i.e., *m*Mg:Ca 5.2 vs 2.5 and 5.2 vs 1.5), differentially expressed genes with p-value < 0.01 and log-fold changes - 2 > and > 2 were considered. The complete DESeq2 R workflow, along with the count matrices, expression

tables, and sequences of differentially expressed genes are available as supplementary materials at https://github.com/PalMuc/CalciteSea.

Results

Mineralogical Analysis

Mineralogical analysis of *Heliopora coerulea* and *Montipora digitata* skeletons showed species-specific responses to variations in seawater *m*Mg:*m*Ca (Figure 2a). Under control conditions (*m*Mg:*m*Ca = 5.2) and *m*Mg:*m*Ca of 2.5, no calcite could be detected in both *H. coerulea* and *M. digitata* (Figure 2), with this pattern being consistent between the two experimental replicates. Contrary, the presence of calcite was detected in one *M. digitata* coral sample maintained under calcite-inducing conditions (*m*Mg:*m*Ca of 1.5), whereas only aragonite was observed in the *H. coerulea* skeleton areas surveyed under these conditions.

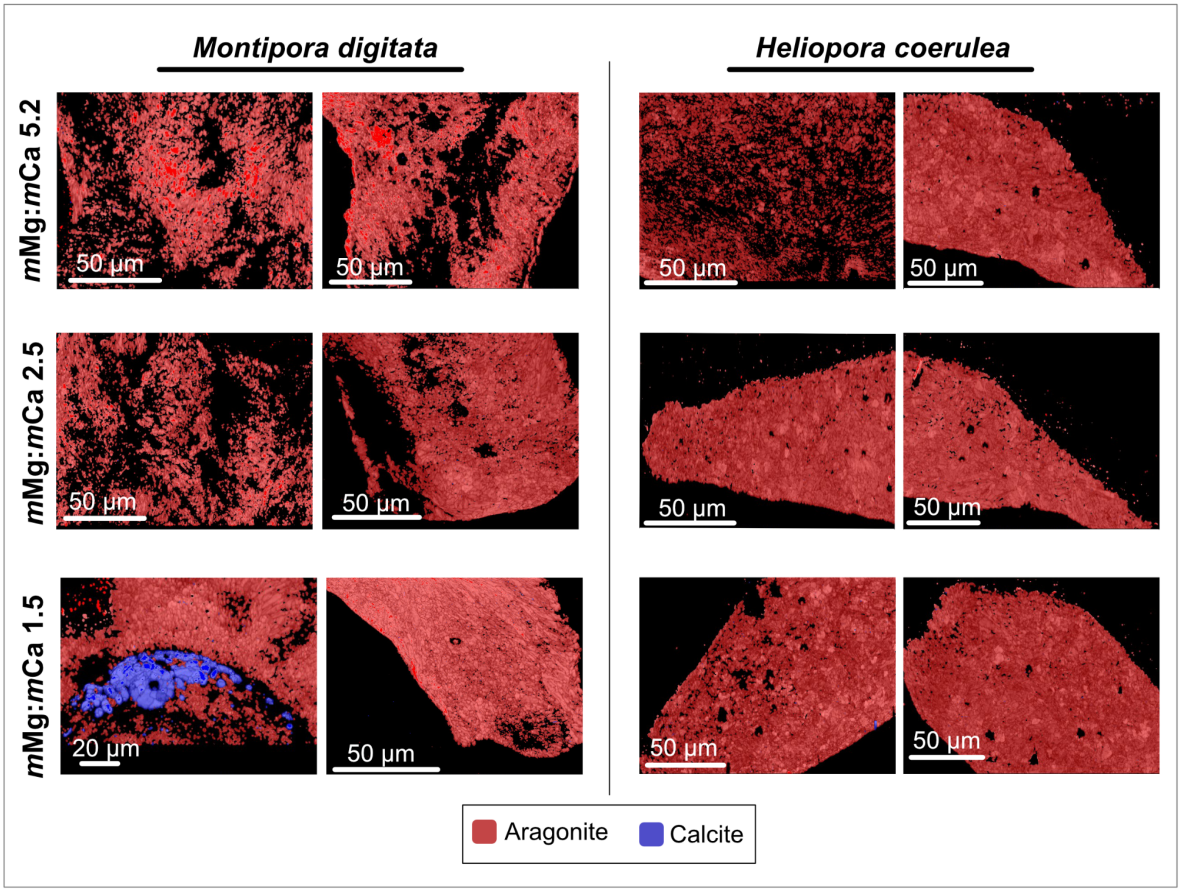

Figure 2: Phase map of *Montipora digitata* and *Heliopora coerulea* skeletons grown under *m*Mg:*m*Ca 5.2, 2.5 and 1.5. Red color = aragonite, Blue color = calcite.

Microscopy imaging (Figure 3a, 3b) shows that the calcite did not form homogeneously within the newly deposited skeleton, but it was rather found restricted within mineral circular micrometric structures. These appear in turn to be in direct contact with the coral skeleton. Phase analysis (Figure 2, 3c, 3d) revealed a mixed composition within these areas with the co-presence of both aragonite and calcite. Neither these circular structures (Figure 3a) nor calcite (Figure S1) could be detected in the portion of the skeleton grown prior to the experiment.

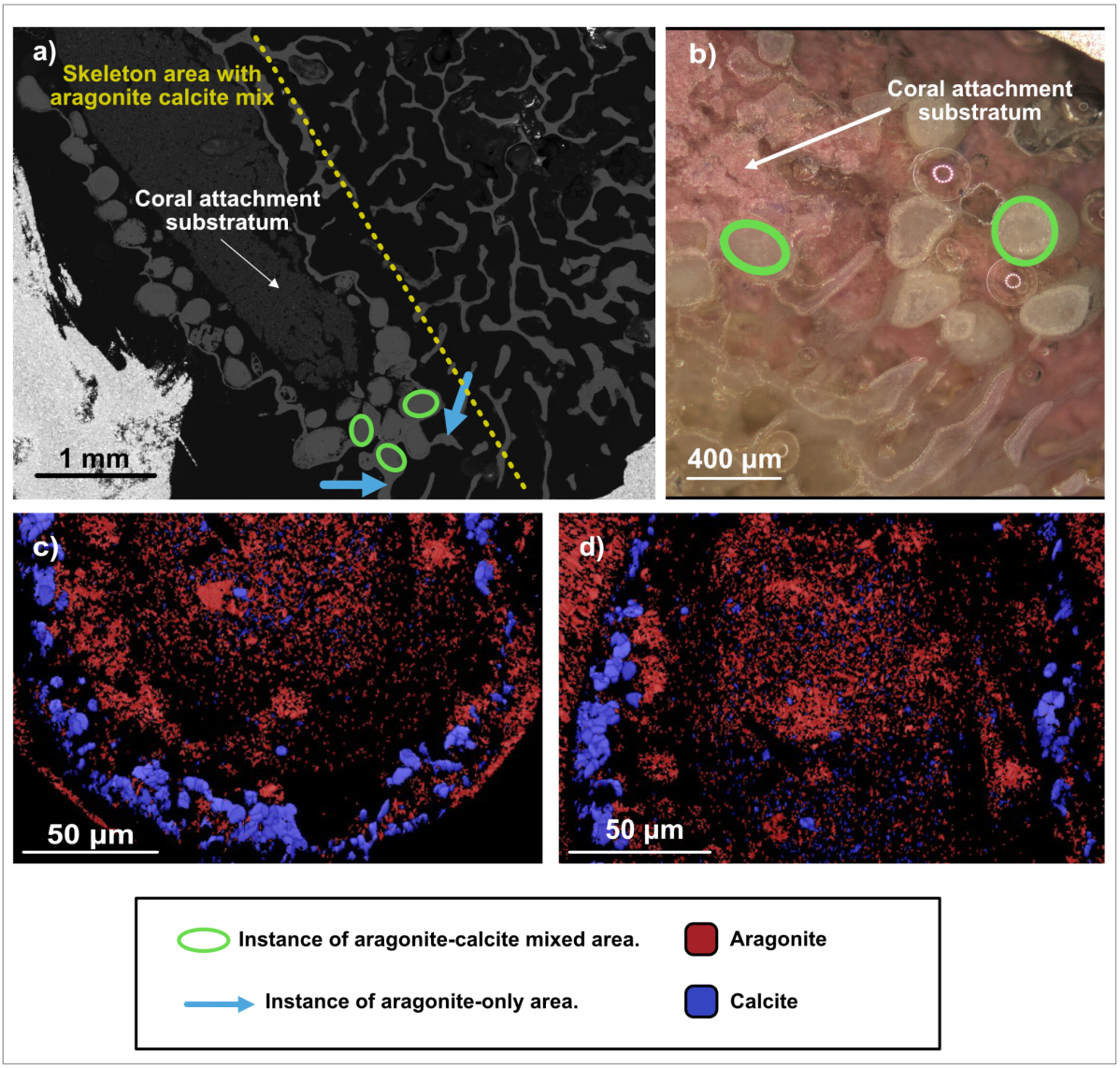

Figure 3: a) Scanning electron microscopy image (backscatter) of *M. digitata* skeleton grown under *m*Mg:*m*Ca of 1.5. Yellow dashed line indicates the boundary between the skeleton grown before and after the start of the experiment. **b)** Light microscopy image of *M. digitata* skeleton grown under *m*Mg:*m*Ca of 1.5. **c)** and **d)** EBSD phase maps showing distribution of calcite (blue) and aragonite (red) within "mixed" areas (green circles).

Analysis of grain area and diameters showed differences between species, experimental conditions, and replicates (Figure S2 and S3). In *M. digitata*, no difference in terms of grain area or both major and minor grain axes in corals exposed to *m*Mg:*m*Ca of 2.5, while in one coral grown at *m*Mg:*m*Ca of 1.5 a decrease in grain size - compared to control conditions - could be observed. On the contrary, in one experiment replicate both corals grown under treatment conditions (2.5 and 1.5) exhibited larger grain sizes. For both species, differences between control and treatment ratios were larger when grain areas were compared, while a higher overlap could be observed when comparing the grain minor axis.

Gene Expression Analysis

Exposure to *m*Mg:*m*Ca ratios of 2.5 and 1.5 triggered changes in gene expression (p-value < 0.001; log fold change > |2|) in both species. The octocoral *H. coeruela* showed higher numbers of differentially expressed genes (DEGs) compared to *M. digitata* under both treatments. Principal component analysis (PCA), based on log-transformed expression values relative to control, revealed, however, a high dispersion of control and treatment samples of *M. digitata,* and strong differences between experimental replicates (Figures S5 and S6). For both species, a set of genes changed expression in both treatments, but several DEGs (both over and underexpressed) were found to be unique to either *m*Mg:*m*Ca ratios of 2.5 or 1.5.

In *M. digitata*, expression changes of known putative calcification-related genes were restricted to *m*Mg:*m*Ca of 1.5. These included the over-expression of one galaxin-like 2 (AD50285.1) homolog, one matrix metalloproteinase-like protein and one uncharacterized skeletal matrix protein (B3EX00.1) previously identified in the skeleton of *Acropora millepora* (Ramos-Silva et al., 2013)

Table 2. Putative calcification-related genes that exhibited changes in expression during both experimental replicates. LFC: Log Fold Change, Padj: adjusted p-value.

Sequence ID	Annotation	Species	*m*Mg:*m*Ca	LFC / Padj
TransAbySS.k25.R1644600.p1	Unch. skeletal matrix protein 1-like	*M. digitata*	1.5	2.57 / < 0.01
Trinity_DN1436_c0_g1_i9.p1	Galaxin-like 2	*M. digitata*	1.5	2.00 / < 0.01
Trinity_DN121764_c0_g1_i3.p1	Metalloproteinase 25-like	*M. digitata*	1.5	2.11 / < 0.01
SOAP.k25.C2929031.p1	Cartilage-intermediate-layer protein-like	*H.coerulea*	2.5	-10 / < 0.01

In *H. coerulea,* the only putative calcification DEG found coded for a cartilage-intermediate layer like-protein and was consistently down-regulated in blue corals exposed to *m*Mg:*m*Ca of 2.5. However, several possible calcification-related genes were differentially expressed in experimental replicate one. These included one protocadherin fat4-like protein - reported from the skeleton of *A. millepora (Ramos-Silva et al., 2013)*. Although changes in the expression of calcium or magnesium transporters was not detected in both experimental replicates, different voltage-dependant calcium channel alpha subunits (matching L, N and T-type channels), transient receptor potential channel-like proteins, and one mitochondrial proton/calcium exchanger-like gene were down-regulated in *H. coerulea* under *m*Mg:*m*Ca of 2.5 in Experiment 1.

Discussion

The formation of coral skeletons is intimately linked to both cellular/molecular processes, and the surrounding environmental conditions. Among the latter, the magnesium/calcium molar ratio of seawater (*m*Mg:*m*:Ca) appears to have influenced the polymorph of calcium carbonate ($CaCO_3$) of major marine calcifiers, and the polymorph initially adopted by marine organisms during the last 500 myr (Zhuravlev and Wood, 2008). However, organisms also appear to be less affected by subsequent changes in seawater chemistry promoting the precipitation of a different polymorph (Porter, 2010). Manipulative experiments conducted in artificially recreated Calcite Seas have, however, highlighted the inability of modern scleractinian corals to fully counteract the effects of *m*Mg:*m*Ca changes, leading to significant amounts of calcite being deposited within their skeletons (Ries et al., 2006; Higuchi et al., 2014). This study combined mineralogical (electron backscattered diffraction, EBSD) and molecular (gene expression) analyses to provide a first insight on the effect of different Mg:Ca molar ratios on aragonitic octocoral skeletons, namely those of *Heliopora coerulea*, and compared the results with the scleractinian coral *Montipora digitata*. To examine and compare their responses at the polymorph and gene expression level, both species were exposed to three different *m*Mg:*m*Ca ratios: the modern value of 5.2 (control group), 2.5 and 1.5.

These experiments highlighted a species-specific response of the corals at *m*Mg:*m*:Ca ratio of 1.5, with significant amounts of calcite being detected in one *M. digitata* sample investigated and none in *H. coerulea.* As in the octocoral species, however, aragonite remained the main component of the *M. digitata* skeleton under all conditions tested. Our

results in *M. digitata* are concordant with previous investigations on this and other species (Ries et al., 2006; Higuchi et al., 2014; Yuyama and Higuchi, 2019), although we could not observe calcite at higher *m*Mg:*m*Ca ratios as previously described in *M. digitata* (Ries et al., 2006). In this regard, differences in the experimental setup, analytical methods and both coral target species and life stage have nonetheless to be considered when comparing results across different studies. In addition, our CaCO3 polymorph characterization (EBSD) was restricted to delimited areas of the coral colonies possibly causing an underestimation of total calcite content of the skeletons of the two species.

The origin and formation mechanisms of the calcite observed at low *m*Mg:*m*Ca ratios in *M.digitata* remain elusive. The distribution analysis of the detected calcite grains point to the calcite-inducing effects of the *m*Mg:*m*Ca ratio not being limited to polymorph substitutions (same structure but different composition), as calcite was only observed in areas which exhibit distinct macro-morphological differences compared to the rest of the skeleton. In this regard, although the observed morphological variation could be related to the effects of *m*Mg:*m*Ca on the biological calcification machinery, we consider more likely that the observed structures originate in enclosed areas of *M. digitata*'s skeleton when corals are exposed to calcite-inducing conditions. In these chambers the composition of calcification fluids can experience strong shifts and promote the precipitation of calcite alongside aragonite. Finally, it cannot be excluded that the presence of calcite could also be possibly related to other mechanisms, such as presence of foreign mineral material, that has been observed in scleractinian skeletons (Goffredo et al., 2012).

In this study, the investigation of possible molecular mechanisms behind the effects of *m*Mg:*m*Ca on coral calcification were hampered by the strong variability observed between experiments. Expression data from *H. coerulea* highlighted expression changes – consistent across experiments – for only one putative calcification related gene: one cartilage-intermediate layer protein homolog underexpressed under *m*Mg:*m*Ca of 2.5. No expression changes for components of the known skeleton proteome of this species (Conci et al., 2020) was detected. On the other hand, in *M. digitata*, a set of calcification-related genes – including a galaxin-related protein – was found upregulated in both experimental replicates. The response of SkOM genes to calcite-inducing *m*Mg:*m*Ca described here might nonetheless have been underestimated, as the high variability observed between and within experiments for *M. digitata* might have prevented us from detecting changes in the expression of additional genes. Overexpression of multiple SkOM proteins under

calcite-inducing *m*Mg:*m*Ca has been reported in *A. tenuis*, and was linked to active initiation and maintenance of aragonite deposition under adverse environmental conditions (Yuyama and Higuchi, 2019). In addition, in this species genes involved in stress response were differentially expressed in corals exposed to calcite inducing *m*Mg:*m*Ca ratios. Although potentially masked by expression variability within treatment conditions, no pattern of stress response could be identified here. Generally, the overexpression of calcification related genes in corals exposed to calcite inducing environments may indicate an increased energetic expenditure by the corals and explain the decline in calcification rates observed in different coral species at lower *m*Mg:*m*Ca ratios (Higuchi et al., 2014; Ries et al., 2006). The reduction in grain sizes observed here in *M. digitata* may also represent a consequence of a higher energetic cost of calcification under low mMg:mCa ratios. However, as for the gene expression analyses, the level of variation observed across experiments and possible effects of biological variability and sample preparation on the measured grain parameters prompt the need for additional research.

In addition to SkOM components, variation in *m*Mg:*m*Ca ratios could also potentially affect ion transport and/or chemistry of the calcification fluids. Although inconsistent between experiments, the change in expression of calcium transporters in *H. coerulea* could be related to a response of the ion transport machinery used by corals for calcification. An involvement of calcium transporters has been excluded for *A. tenuis,* as no change in expression was detected (Yuyama and Higuchi, 2019). However, in that study the seawater *m*Mg:*m*Ca was manipulated by decreasing [Mg^{2+}], while keeping [Ca^{2+}] at normal levels (ca. 10mM). Thus, information on putative response of calcium and other ions transporters in corals concurrently exposed to low [Mg^{2+}] and increased [Ca^{2+}] is currently lacking. In corals, calcium is supposedly transported to the calcification sites either paracellularly (Gagnon et al., 2012) or via an active transcellular transport (Tanbutté et al., 1996; Hohn and Merico, 2015). Different transporters have been associated with calcium transcellular transport including calcium channels, Ca^{2+}-ATPases and proton exchangers (Zoccola et al., 1999, 2004; Barott et al., 2015; Barron et al., 2018). The regulation of calcium transport allows corals to maintain higher calcium concentration in calcifying fluids ($[Ca^{2+}]_{cf}$) with respect to seawater (Sevilgen et al., 2019). Up-regulation of $[Ca^{2+}]_{cf}$ can also be enhanced in some coral species to counteract decreases in the saturation state of the calcifying medium caused by decreases in seawater pH (DeCarlo et al., 2018). Different studies have in fact examined the effects of ocean acidification on carbonate and calcium chemistry at calcification sites (Allison et al., 2018; Mollica et al., 2018). However, to the best of our

knowledge, research examining the response of ion transport to the calcification site when the environmental calcium concentration is higher than $[Ca^{2+}]_{cf}$ is currently lacking. Further characterizations of the calcium transport machinery in octocorals and scleractinian in the future could nonetheless provide additional insights on the localization and role of single calcium channels, and possibly corroborating the hypothesis that corals might control aragonite precipitation, when exposed to high environmental $[Ca^{2+}]$, through the regulation of calcium transport.

Here, we documented changes in skeleton polymorph and in the expression of calcification-related genes in the aragonitic octocoral *H. coerulea* and the scleractinian *M. digitata* exposed to calcite-inducing *m*Mg:*m*Ca. This work provides the first comparative study of octocoral and scleractinian responses to changes in *m*Mg:*m*Ca. The two species were found to respond differently with calcite not being detected in the skeleton of *H. coerulea,* while present in *M. digitata.* Despite strong variability both within and between experiments, changes in gene expression point to an involvement of SkOM genes and, potentially, calcium transporters in the response of calcifying anthozoans to different *m*Mg:*m*Ca.

Acknowledgements:

The study was supported by the German Research Foundation (DFG) grant “MINORCA” to S.V. (Project Number Va1146-2/1) and G.W. (Project Number Wo896/18-1). G.W. acknowledges support by LMU Munich’s Institutional Strategy LMUexcellent within the framework of the German Excellence Initiative. We thank Dr Peter Naumann for technical assistance and maintenance of the aquaria facilities and coral culturing, as well as Simone Schätzle and Gabriele Büttner for assistance in the laboratory and Moritz Zenkert for EBSD samples preparation.

References

Allison, N., Cole, C., Hintz, C., Hintz, K., Rae, J., and Finch, A.: The effect of ocean acidification on tropical coral calcification: Insights from calcification fluid DIC chemistry, Chem. Geol., 497, 162–169, 2018.

Balthasar, U. and Cusack, M.: Aragonite-calcite seas—Quantifying the gray area, Geology, 43, 99–102, 2015.

Barott, K. L., Perez, S. O., Linsmayer, L. B., and Tresguerres, M.: Differential localization of ion transporters suggests distinct cellular mechanisms for calcification and photosynthesis

between two coral species, Am. J. Physiol. Regul. Integr. Comp. Physiol., 309, R235–46, 2015.

Barron, M. E., Thies, A. B., Espinoza, J. A., Barott, K. L., Hamdoun, A., and Tresguerres, M.: A vesicular Na+/Ca2+ exchanger in coral calcifying cells, PLoS One, 13, e0205367, 2018.

Bertucci, A., Tambutté, S., Supuran, C. T., Allemand, D., and Zoccola, D.: A new coral carbonic anhydrase in *Stylophora pistillata*, Mar. Biotechnol., 13, 992–1002, 2011.

Chomczynski, P. and Mackey, K.: Short technical reports. Modification of the TRI reagent procedure for isolation of RNA from polysaccharide- and proteoglycan-rich sources, Biotechniques, 19, 942–945, 1995.

Colgan, M. W.: The Cretaceous Coral *Heliopora* (Octocorallia, Coenothecalia)—a Common Indo-Pacific Reef Builder, in: Living Fossils, edited by: Eldredge, N. and Stanley, S. M., Springer New York, New York, NY, 266–271, 1984.

Conci, N., Lehmann, M., Vargas, S., and Wörheide, G.: Comparative proteomics of octocoral and scleractinian skeletomes and the evolution of coral calcification, Genome Biol. Evol., 12, 1623–1635, 2020.

DeCarlo, T. M., Comeau, S., Cornwall, C. E., and McCulloch, M. T.: Coral resistance to ocean acidification linked to increased calcium at the site of calcification, Proc. Biol. Sci., 285, 2018.

Dunn, C. W., Howison, M., and Zapata, F.: Agalma: an automated phylogenomics workflow, BMC Bioinformatics, 14, 330, 2013.

Eguchi, M.: Fossil Helioporidae from Japan and the South Sea Islands, J. Paleontol., 22, 362–364, 1948.

Gagnon, A. C., Adkins, J. F., and Erez, J.: Seawater transport during coral biomineralization, Earth Planet. Sci. Lett., 329-330, 150–161, 2012.

Goffredo, S., Vergni, P., Reggi, M., Caroselli, E., Sparla, F., Levy, O., Dubinsky, Z., and Falini, G.: The skeletal organic matrix from Mediterranean coral *Balanophyllia europaea* influences calcium carbonate precipitation, PLoS One, 6, e22338, 2011.

Goffredo, S., Caroselli, E., Mezzo, F., Laiolo, L., Vergni, P., Pasquini, L., Levy, O., Zaccanti, F., Tribollet, A., Dubinsky, Z., and Falini, G.: The puzzling presence of calcite in skeletons of modern solitary corals from the Mediterranean Sea, Geochim. Cosmochim. Acta, 85, 187–199, 2012.

Grabherr, M. G., Haas, B. J., Yassour, M., Levin, J. Z., Thompson, D. A., Amit, I., Adiconis, X., Fan, L., Raychowdhury, R., Zeng, Q., Chen, Z., Mauceli, E., Hacohen, N., Gnirke, A., Rhind, N., di Palma, F., Birren, B. W., Nusbaum, C., Lindblad-Toh, K., Friedman, N., and Regev, A.: Full-length transcriptome assembly from RNA-Seq data without a reference genome, Nat. Biotechnol., 29, 644–652, 2011.

Higuchi, T., Fujimura, H., Yuyama, I., Harii, S., Agostini, S., and Oomori, T.: Biotic control of skeletal growth by scleractinian corals in Aragonite–Calcite Seas, PLoS One, 9, e91021, 2014.

Hohn, S. and Merico, A.: Quantifying the relative importance of transcellular and paracellular

ion transports to coral polyp calcification, Front. Earth Sci., 2, 1129, 2015.

Hohn, S. and Reymond, C. E.: Coral calcification, mucus, and the origin of skeletal organic molecules, Coral Reefs, 38, 973–984, 2019.

Janiszewska, K., Mazur, M., Escrig, S., Meibom, A., and Stolarski, J.: Aragonitic scleractinian corals in the Cretaceous calcitic sea, Geology, 45, 319–322, 2017.

Laipnik, R. ’anan, Bissi, V., Sun, C.-Y., Falini, G., Gilbert, P. U. P. A., and Mass, T.: Coral acid rich protein selects vaterite polymorph in vitro, J. Struct. Biol., 107431, 2019.

Le Goff, C., Ganot, P., Zoccola, D., Caminiti-Segonds, N., Allemand, D., and Tambutté, S.: Carbonic Anhydrases in Cnidarians: Novel Perspectives from the octocorallian *Corallium rubrum*, PLoS One, 11, e0160368, 2016.

Love, M. I., Huber, W., and Anders, S.: Moderated estimation of fold change and dispersion for RNA-seq data with DESeq2, Genome Biol., 15, 550, 2014.

Lowenstam, H. A. and Weiner, S.: On biomineralization, 1989.

Mollica, N. R., Guo, W., Cohen, A. L., Huang, K.-F., Foster, G. L., Donald, H. K., and Solow, A. R.: Ocean acidification affects coral growth by reducing skeletal density, Proc. Natl. Acad. Sci. U. S. A., 115, 1754–1759, 2018.

Morse, J. W. and Mackenzie, F. T.: Geochemistry of Sedimentary Carbonates, Elsevier, 706 pp., 1990.

Morse, J. W., Wang, Q., and Tsio, M. Y.: Influences of temperature and Mg:Ca ratio on CaCO3 precipitates from seawater, Geology, 25, 85–87, 1997.

Moya, A., Tambutté, S., Bertucci, A., Tambutté, E., Lotto, S., Vullo, D., Supuran, C. T., Allemand, D., and Zoccola, D.: Carbonic anhydrase in the scleractinian coral *Stylophora pistillata*: characterization, localization, and role in biomineralization, J. Biol. Chem., 283, 25475–25484, 2008.

Patro, R., Duggal, G., Love, M. I., Irizarry, R. A., and Kingsford, C.: Salmon provides fast and bias-aware quantification of transcript expression, Nat. Methods, 14, 417–419, 2017.

Peled-Kamar, M., Hamilton, P., and Wilt, F. H.: Spicule matrix protein LSM34 is essential for biomineralization of the sea urchin spicule, Exp. Cell Res., 272, 56–61, 2002.

Porter, S. M.: Calcite and aragonite seas and the de novo acquisition of carbonate skeletons, Geobiology, 8, 256–277, 2010.

Puverel, S., Tambutté, E., Pereira-Mouriès, L., Zoccola, D., Allemand, D., and Tambutté, S.: Soluble organic matrix of two Scleractinian corals: partial and comparative analysis, Comp. Biochem. Physiol. B Biochem. Mol. Biol., 141, 480–487, 2005.

Rahman, M. A. and Oomori, T.: In Vitro Regulation of CaCO3 Crystal Growth by the Highly Acidic Proteins of Calcitic Sclerites in Soft Coral, *Sinularia polydactyla*, Connect. Tissue Res., 50, 285–293, 2009.

Ramos-Silva, P., Kaandorp, J., Huisman, L., Marie, B., Zanella-Cléon, I., Guichard, N., Miller, D. J., and Marin, F.: The skeletal proteome of the coral *Acropora millepora*: the evolution of

calcification by co-option and domain shuffling, Mol. Biol. Evol., 30, 2099–2112, 2013.

Randle, V. and Engler, O.: Introduction to Texture Analysis: Macrotexture, 125–151, 2000.

Reggi, M., Fermani, S., Samorì, C., Gizzi, F., Prada, F., Dubinsky, Z., Goffredo, S., and Falini, G.: Influence of intra-skeletal coral lipids on calcium carbonate precipitation, CrystEngComm, 18, 8829–8833, 2016.

Ries, J. B., Stanley, S. M., and Hardie, L. A.: Scleractinian corals produce calcite, and grow more slowly, in artificial Cretaceous seawater, Geology, 34, 525–528, 2006.

Rivera-Vicéns, R. E., Garcia-Escudero, C. A., Conci, N., Eitel, M., and Wörheide, G.: TransPi-a comprehensive TRanscriptome ANalysiS PIpeline for de novo transcriptome assembly, Mol. Ecol. Resour., https://doi.org/10.1111/1755-0998.13593, 2022.

Sandberg, P. A.: An oscillating trend in Phanerozoic non-skeletal carbonate mineralogy, Nature, 305, 19–22, 1983.

Schmidt, N.-H. and Olesen, N. O.: Computer-aided determination of crystal-lattice orientation from electron channeling patterns in the SEM, Can. Mineral., 27, 15–22, 1989.

Sevilgen, D. S., Venn, A. A., Hu, M. Y., Tambutté, E., de Beer, D., Planas-Bielsa, V., and Tambutté, S.: Full in vivo characterization of carbonate chemistry at the site of calcification in corals, Sci Adv, 5, eaau7447, 2019.

Shinzato, C., Shoguchi, E., Kawashima, T., Hamada, M., Hisata, K., Tanaka, M., Fujie, M., Fujiwara, M., Koyanagi, R., Ikuta, T., Fujiyama, A., Miller, D. J., and Satoh, N.: Using the *Acropora digitifera* genome to understand coral responses to environmental change, Nature, 476, 320–323, 2011.

Simão, F. A., Waterhouse, R. M., Ioannidis, P., Kriventseva, E. V., and Zdobnov, E. M.: BUSCO: assessing genome assembly and annotation completeness with single-copy orthologs, Bioinformatics, 31, 3210–3212, 2015.

Stanley, S. M. and Hardie, L. A.: Secular oscillations in the carbonate mineralogy of reef-building and sediment-producing organisms driven by tectonically forced shifts in seawater chemistry, Palaeogeogr. Palaeoclimatol. Palaeoecol., 144, 3–19, 1998.

Stanley, S. M. and Hardie, L. A.: Hypercalcification: paleontology links plate tectonics and geochemistry to sedimentology, GSA Today, 9, 1–7, 1999.

Stolarski, J., Meibom, A., Przenioslo, R., and Mazur, M.: A Cretaceous scleractinian coral with a calcitic skeleton, Science, 318, 92–94, 2007.

Stolarski, J., Coronado, I., and Murphy, J. G.: A modern scleractinian coral with a two-component calcite–aragonite skeleton, 2021.

Tanbutté, É., Allemand, D., Mueller, E., and Jaubert, J.: A compartmental approach to the mechanism of calcification in hermatypic corals, J. Exp. Biol., 199, 1029–1041, 1996.

Thompson, J. B., Paloczi, G. T., Kindt, J. H., Michenfelder, M., Smith, B. L., Stucky, G., Morse, D. E., and Hansma, P. K.: Direct observation of the transition from calcite to aragonite growth as induced by abalone shell proteins, Biophys. J., 79, 3307–3312, 2000.

Von Euw, S., Zhang, Q., Manichev, V., Murali, N., Gross, J., Feldman, L. C., Gustafsson, T.,

Flach, C., Mendelsohn, R., and Falkowski, P. G.: Biological control of aragonite formation in stony corals, Science, 356, 933–938, 2017.

Wheeler, A. P., George, J. W., and Evans, C. A.: Control of calcium carbonate nucleation and crystal growth by soluble matrx of oyster shell, Science, 212, 1397–1398, 1981.

Yuyama, I. and Higuchi, T.: Differential gene expression in skeletal organic matrix proteins of scleractinian corals associated with mixed aragonite/calcite skeletons under low mMg/Ca conditions, PeerJ, 7, e7241, 2019.

Zhuravlev, A. Y. and Wood, R. A.: Eve of biomineralization: Controls on skeletal mineralogy, Geology, 36, 923–926, 2008.

Zoccola, D., Tambutté, E., Sénégas-Balas, F., Michiels, J. F., Failla, J. P., Jaubert, J., and Allemand, D.: Cloning of a calcium channel alpha1 subunit from the reef-building coral, *Stylophora pistillata*, Gene, 227, 157–167, 1999.

Zoccola, D., Tambutté, E., Kulhanek, E., Puverel, S., Scimeca, J.-C., Allemand, D., and Tambutté, S.: Molecular cloning and localization of a PMCA P-type calcium ATPase from the coral *Stylophora pistillata*, Biochim. Biophys. Acta, 1663, 117–126, 2004.

Zoccola, D., Ganot, P., Bertucci, A., Caminiti-Segonds, N., Techer, N., Voolstra, C. R., Aranda, M., Tambutté, E., Allemand, D., Casey, J. R., and Tambutté, S.: Bicarbonate transporters in corals point towards a key step in the evolution of cnidarian calcification, Sci. Rep., 5, 9983, 2015.

Supplementary Figures

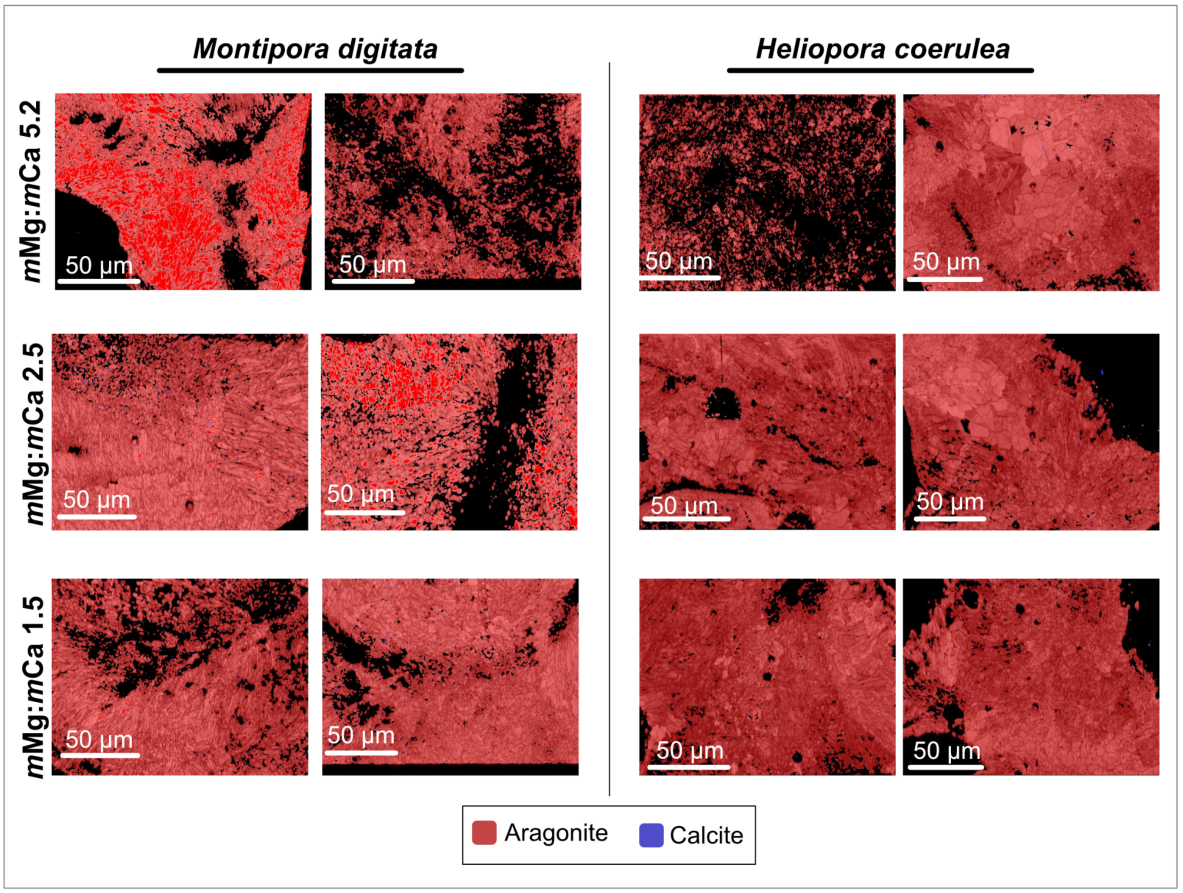

Figure S1: Phase map of *Montipora digitata* and *Heliopora coerulea* skeletons grown before the start of the experiments.. Red color = aragonite, Blue color = calcite.

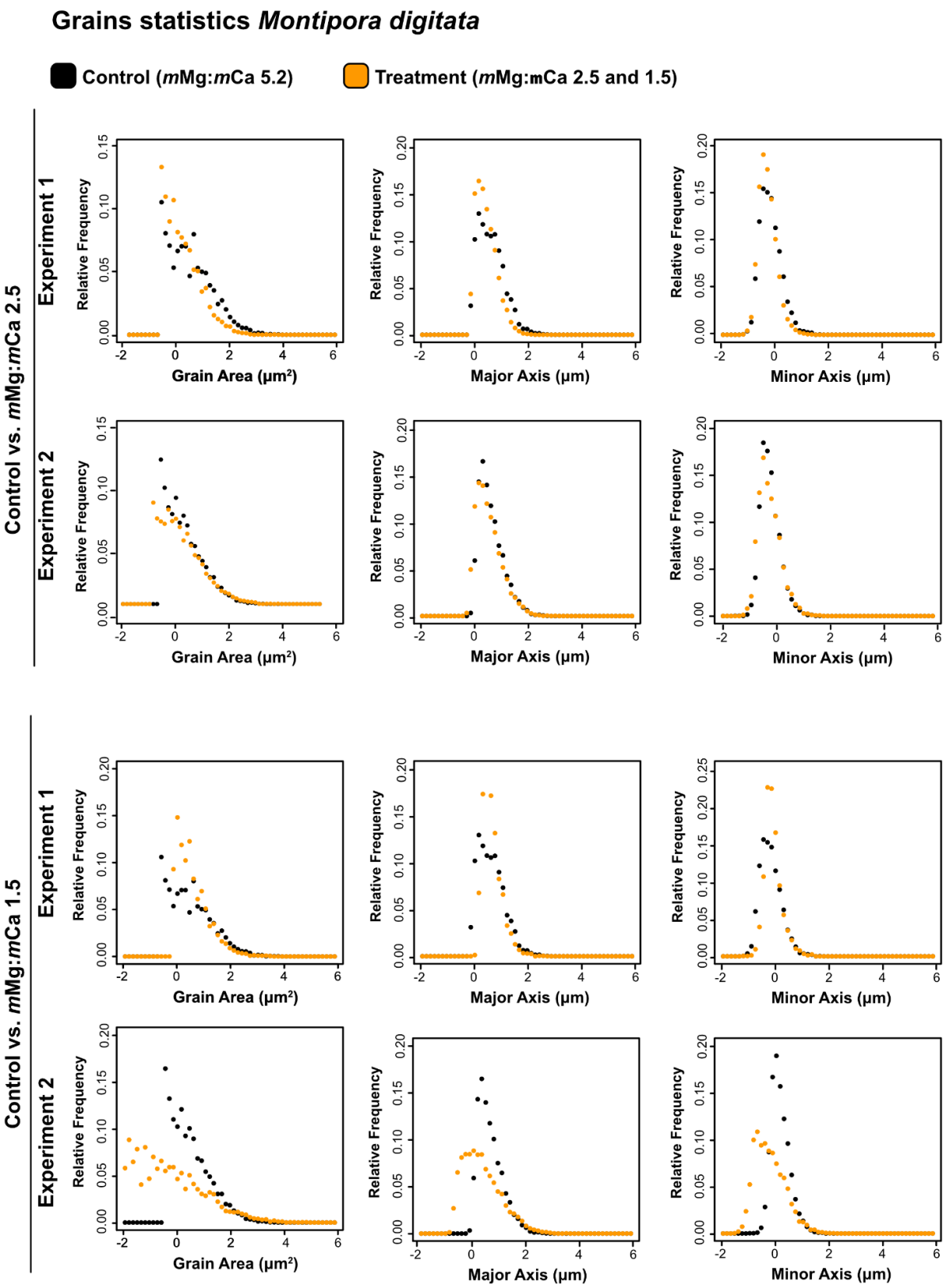

Figure S2: Frequency distribution of grain area, major and minor axis (log transformed) in *Montipora digitata* corals grown under different *m*Mg:*m*Ca during both experimental replicates. Datasets and script to generate plots available as supplementary at https://github.com/PalMuc/CalciteSea.

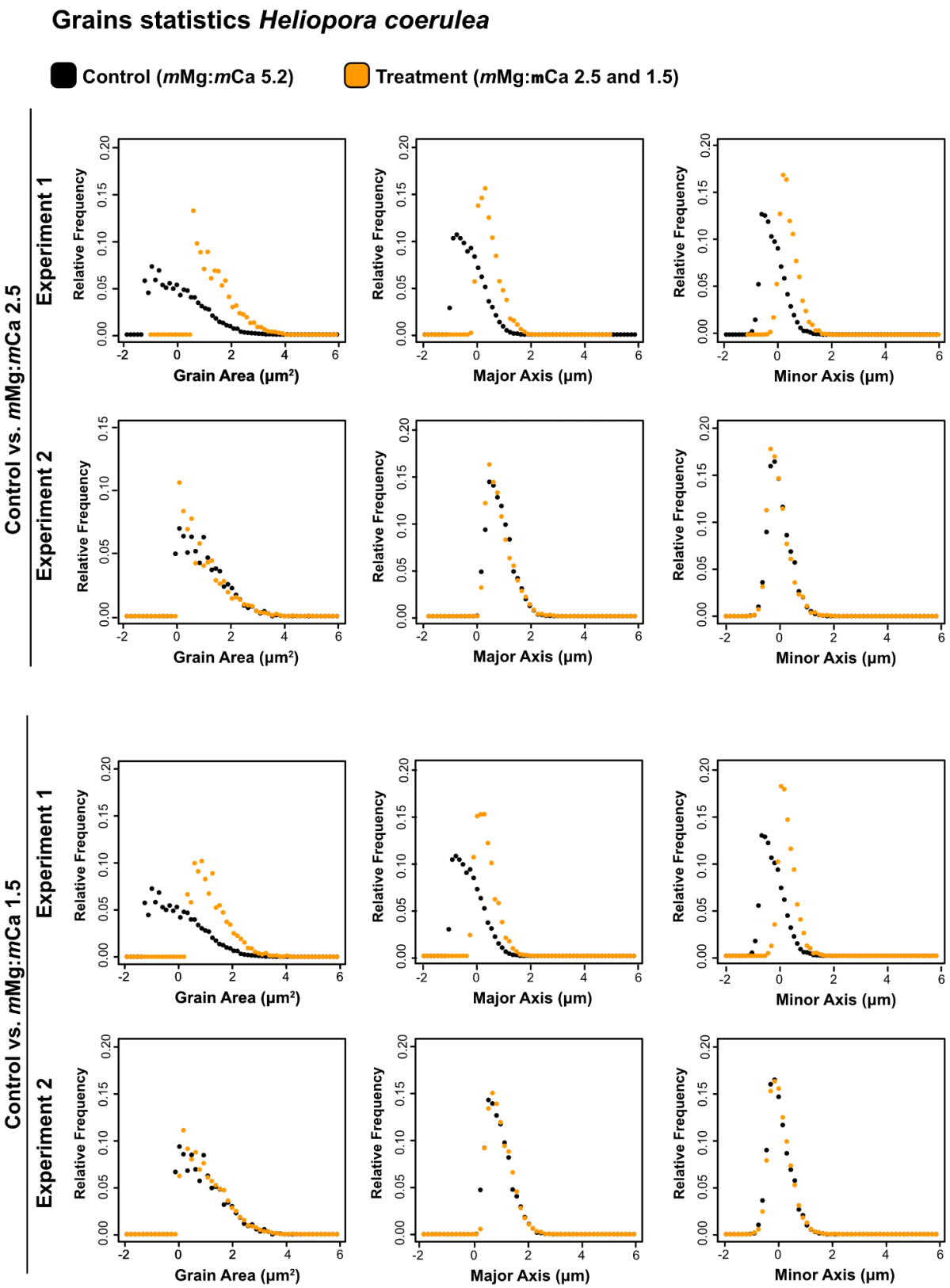

Figure S3: Frequency distribution of grain area, major and minor axis (log transformed) in *Heliopora coerulea* corals grown under different *m*Mg:*m*Ca during both experimental replicates. Datasets and script to generate plots available as supplementary at https://github.com/PalMuc/CalciteSea.

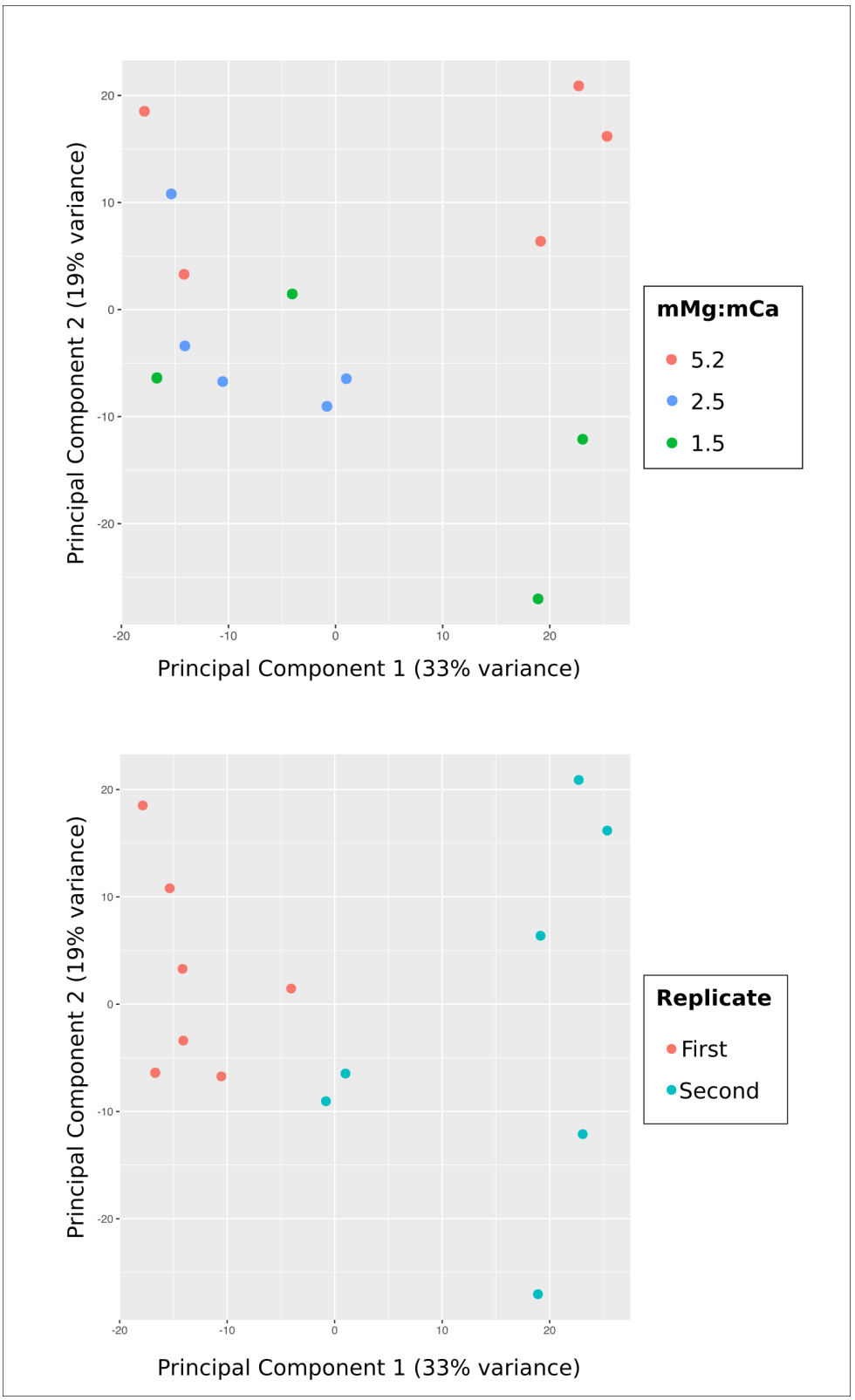

Figure S4: Principal component analysis for expression of genes assigned by psytrans to *M. digitata*. Dots are colored based on experimental condition (*m*Mg:*m*Ca) (top) and experimental replication (bottom).

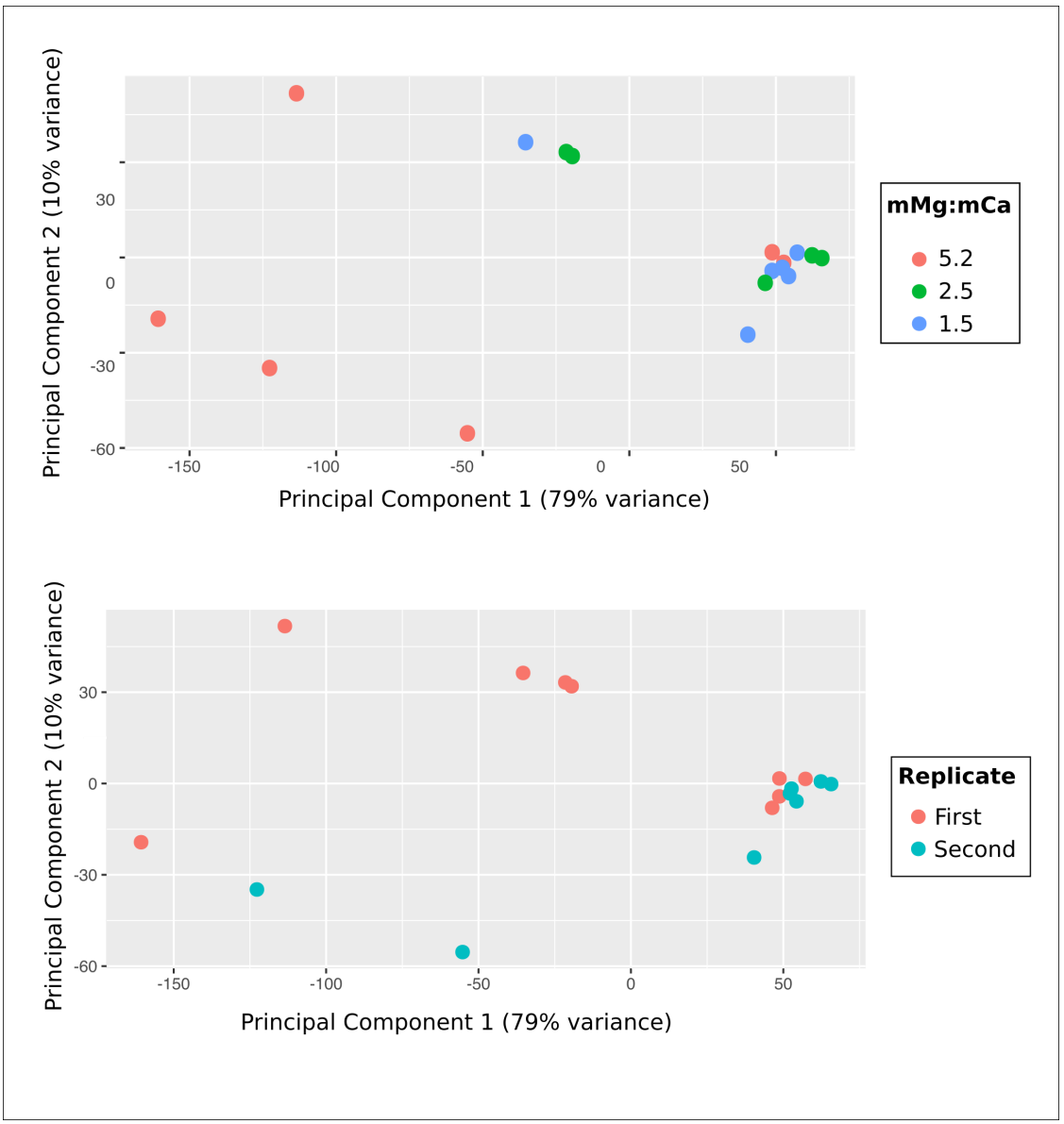

Figure S5: Principal component analysis for expression of genes assigned by psytrans to *M. digitata*. Dots are colored based on experimental condition (*m*Mg:*m*Ca) (top) and experimental replication (bottom).